Discussion Of Failure In Scour Protections

Tiago Fazeres-Ferradosa,[1*] Mario Welzel,[2] Francisco Taveira-Pinto[1], Paulo Rosa-Santos[1], Alemi Mahdi[1], Alexander Schendel[3], Richard J.S. Whitehouse[4]

[1] Faculty of Engineering, University of Porto & CIIMAR - Interdisciplinary Centre of Marine and Environmental Research, 4200-465, Porto, Portugal, email: tferradosa@fe.up.pt; fpinto@fe.up.pt; pjrsantos@fe.up.pt; mahdialemi@yahoo.com

[2] TU Braunschweig, Leichtweiß-Institute for Hydraulic Engineering and Water Resources, Dept. of Hydromechanics, Coastal and Ocean Engineering, Universitätsplatz 2 38106 Braunschweig, P. O. Box: 38092 Braunschweig, Germany. email: mario.welzel@tu-braunschweig.de.

[3] Ludwig-Franzius-Institute for Hydraulic, Estuarine and Coastal Engineering, Leibniz University Hannover, Hannover 30167, Germany. email: schendel@lufi.uni-hannover.de

[4] HR Wallingford, Howbery Park, Wallingford, Oxfordshire, OX10 8BA, United Kingdom. email: R.Whitehouse@hrwallingford.com

Corresponding author: Tiago Fazeres-Ferradosa, tferradosa@fe.up.pt

ABSTRACT

Scour protections are a key aspect to ensure the stability of offshore foundations. However, their cost can represent a considerable portion of the CAPEX and OPEX parcels of an offshore wind investment. Therefore, recent studies have been focused on optimising this component, namely, through the concepts of wide-graded and dynamic scour protections. These optimisations aim at reducing the median stone diameter of the armour layer, while combining this reduction with a suitable thickness of the scour protection. Former studies on these optimisations define failure through a visual criterion, which corresponds to the exposure of the underlying filter layer over an area of four times the median nominal (square shaped) stone area. Visual identification of damage may be difficult during testing, with conditions which often have suspended sediments in the flow or sand gathering on top of the protection. Moreover, it often leads to uncertainty in the assessment of the value of the exposed area. The present research discusses how to precisely identify the exposure of the filter layer or the sand bed, based on the analysis of bathymetric surveys and the thickness reduction of the scour protection. A possible definition of failure, adaptable to scour protections with different thicknesses, is discussed and exemplified for a small set of scour tests performed in a physical model representing a typical protected monopile foundation under waves and current combined.

KEYWORDS: Failure; Scour Protection; Filter Layer; Damage; Bathymetric profiles

INTRODUCTION

Scour protections are a common requirement for bottom-fixed offshore foundations. They avoid major scour occurrence thus ensuring that the free-span and the natural frequency of the structure

remain within the design limits (Mayall *et al.*, 2019). Often such components represent a large portion of the capital expenditures (CAPEX) and of the operation and maintenance expenditures (OPEX). Therefore, its optimisation has been the focus of several studies, *e.g.* den Boon *et al.* (2004), De Vos *et al.* (2012) or Fazeres-Ferradosa *et al.* (2018a).

Most scour protections are designed to ensure that the armour stones remain statically stable. In these cases, the median stone diameter of the placed rock material is chosen so that its critical shear-stress is not surpassed by the amplified bed shear-stress at the foundations' vicinity. Such design procedure is fully detailed in Whitehouse (1998).

Another possibility is to design the scour protection with a dynamic approach, based on the damage number, S_{3D}. In this approach, the rock is allowed for a controlled degree of movement (see De Vos *et al.*, 2012). Such an approach leads to smaller median stone sizes and, for stability purposes and filter performance, it may be coupled with a larger thickness of the scour protection. The optimisation obtained on the median stone diameter may lead to improved cost-benefit ratios as long as the increase in the volume of material required by the larger thickness is acceptable to the project. If the OPEX parcel is properly accounted throughout the structure's life cycle, dynamic scour protections can lead to a direct cost reduction in the CAPEX parcel.

De Vos *et al.* (2012) proposes that the damage number is calculated from the bathymetric profile of the scour protection, by dividing it into sub-areas, A_{sub}, which are equal to the monopile cross-section area. The damage number at each sub-area, S_{3Dsub}, is obtained by,

$$S_{3D} = \frac{V_e}{D_{n50}\, A_{sub}} = \frac{V_e}{D_{n50}\left(\pi \frac{D_p^2}{4}\right)} \tag{1}$$

where V_e is the eroded volume over A_{sub}, D_{n50} is the median nominal stone diameter and D_p is the pile diameter of a monopile foundation, commonly used in offshore wind turbines.

The representative damage number of the protection, S_{3D}, corresponds to the maximum value occurring in all sub-areas. While in statically stable scour protections the movement of one stone defines the failure occurrence *per se*, in dynamic scour protections De Vos *et al.* (2012) suggest that $S_{3D}=1$ can be adopted as a conservative limit that separates the movement of stones without and with failure.

During the physical modelling activities that led to the development of the dynamic design approach, the tested scour protections were considered to fail if the exposed filter layer exceeded an area of $4D_{50}^2$. This corresponds to the visual criterion introduced in den Boon *et al.* (2004). De Vos *et al.* (2012) found a good agreement with the limit of $S_{3D}=1$ proposed before and den Boon *et al.* (2004).

In fact, this visual identification of failure was successfully adopted in subsequent studies by Fazeres-Ferradosa *et al.* (2018b) and Chavez *et al.* (2019). However, its use might be difficult in common testing conditions, which often have suspended sediments in the flow or sand accumulation on top of the protection. Therefore, accurate ways to evaluate this exposed area of the filter or the sand bottom are an important contribution to an accurate identification of failure.

In the present research, a physical model of a protected monopile foundation, under waves and current combined, is used to present a simple procedure that allows for the mathematical

application of den Boon *et al.* (2004) criterion based on the analysis of bathymetric data. In addition, the interpretation of the damage is discussed in light of the use of the new procedure with a focus on its application to scour protections with different thicknesses.

FAILURE DEFINITION: DAMAGE NUMBER vs. FILTER EXPOSURE

According to De Vos *et al.* (2012), equation 1 presents the average height of stones which has disappeared over the considered sub area, expressed as a function of the nominal stone diameter D_{n50}. When $S_{3Dsub}=1$, this implies that the height of the scour protection has decreased over this sub-area over a distance equal to D_{n50}. In other words, despite the variability of the stone's arrangement in the armour layer, the S_{3D} provides an average measure of the equivalent number of layers of armour stones that are removed over the area A_{sub}.

Considering this interpretation, the filter exposure over A_{sub} requires an S_{3D} larger or equal to the equivalent number of layers of stones existing in the scour protection. For example, a scour protection with a thickness of $3D_{n50}$ would have its underlying filter or bottom sand exposed in any area A_{sub} if its corresponding damage number was equal or greater than 3.

As demonstrated by Schendel et al. (2018) for the case of bed surface degradation, a procedure procedure to mathematically verify the visual failure criterion from den Boon *et al.* (2004) can be defined by applying the De Vos *et al.* (2012) methodology and equation 1 with $A_{sub}=4D_{n50}^2$, instead of using an area equal to the pile cross-section. Then, all values of S_{3Dsub} can be compared with the equivalent number of layers of stones to analyse if the filter is exposed, thus consisting in a failure occurrence. For the example given in the last paragraph: if S_{3Dsub} ($A_{sub=}4D_{n50}^2$) is equal to 3 then the filter is exposed over an area of $4D_{n50}^2$, corresponding to the visual failure criterion (for the nominal median stone diameter). Figure 1 provides a scheme of the arrangement of the circular sub-areas used in this study, in which the size of each sub-area equals $4D_{n50}^2$. The sub-areas arrangement followed a set-up suggested in Fazeres-Ferradosa *et al.* (2019) to fully cover the surface of the scour protection.

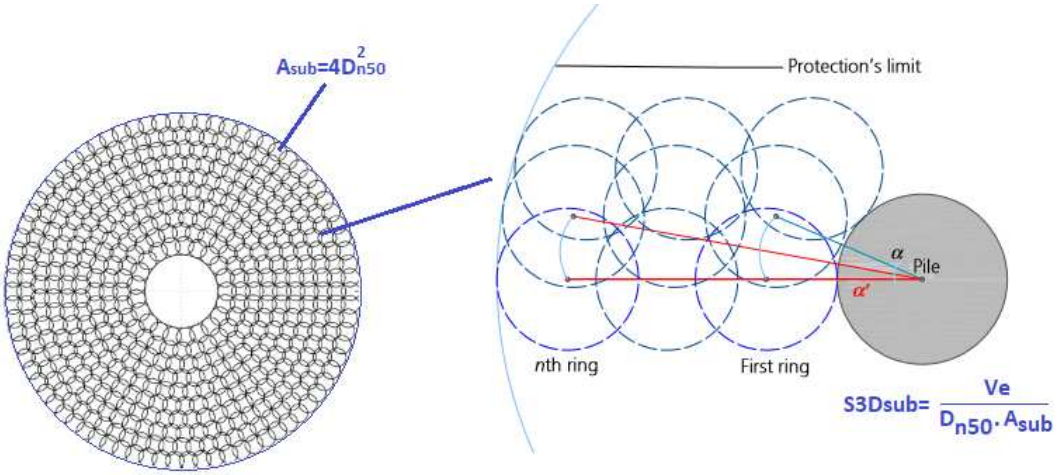

Figure 1. Scheme of overlapping sub-areas used with a size of $4D_{n50}^2$ to mathematically analyse den Boon *et al.* (2004) visual criterion.

The size of the sub-areas influences the range of S_{3D}, thus the values obtained for $A_{sub}=4D_{n50}^2$ are not directly comparable to the ones obtained for $A_{sub}=\pi\times(D_p)^2/4$, even though the physical interpretation is the same. A detailed discussion of this aspect can be found in Fazeres-Ferradosa *et al.* (2019). In the experiments reported by De Vos *et al*. (2012), scour protection thicknesses of $3D_{n50}$ and $2.5D_{n50}$ were tested. Failure was reported for S_{3D}=[1.21; 2.39], which are below the number of layers used. However, we note that these values are the average height of stones which disappeared over the sub-area equal to the monopile diameter which is a much larger area than $4D_{n50}^2$. A potential reason for this apparent contradiction can be the fact that using very wide areas contributes to an attenuation of the value of the damage number, while the exposure of the filter layer can occur in smaller areas. Using A_{sub} equal to the monopile cross-section might be an advantage to implement the dynamic design approach in that it smooths the analysis results, but A_{sub} equal to $4D_{n50}^2$ seems to be a useful value to use when seeking filter or bottom sand exposures. The next section provides the analysis of a set of tests, from the PROTEUS project, performed at the Fast Flow Facility (HR Wallingford – UK) – see Table 1. Details of the physical modelling conditions are fully given in Chavez *et al.* (2019). The bathymetric profiles are analysed under the proposed mathematical application of the den Boon *et al.* (2004) criterion to see if any failure is identified. In addition, the thickness reduction as a percentage of the equivalent number of layers of stones is analysed and compared with the visual damage classification proposed in De Vos *et al.* (2012).

RESULTS AND DISCUSSION

For the experimental tests, the reductions in the thickness of scour protections are analysed for $A_{sub}=4D_{n50}^2$. In these tests the geotextile filter layer had an almost negligible thickness, around 3 mm. Therefore, in practice any reference to a total removal of the scour protection corresponds to the geotextile exposure. In Table 1, the reference sub-area was used to analyse how many sub-areas could be found with a removal of 25%, 50%, 75% and 100% of the overall thickness, *i.e.* a damage of 25%, 50%, 75% and 100% of the protection. In other words, when S_{3Dsub}, at any sub-area, reaches the referred percentages of the equivalent number of layers of stones used at the protection.

All tests showed areas with 25% reduction in thickness whereas the majority of the tests showed a reducing number of sub-areas registering a reduction of 50% and 75% without reaching the total removal of the scour protection (non-failures). However, in these cases, further wave series could be run to understand if such dynamic stability would remain after the action of more waves. The number of sub-areas associated with the reduction of the protection thickness provides an indicator on the degree of the dynamic stability. For example, Tests 10A and 10B register a thickness reduction of 25% in relatively few locations, while Tests 4A and 4B present a reduction range of 25 to 75%, without a determination of failure.

Since present failure criteria of dynamic scour protections are often based on visual damage levels or the visual assessment of the filter (or sand) exposure, it is important to perceive if such measures have a match with the thickness reduction noted in each test. Table 1 shows that scour protections

with visual damage level of 2 (according to De Vos *et al.* (2012) – very limited movement of stones) were associated with a maximum reduction of the protection thickness of 25%. Damage level 3 had a maximum reduction of 75%, whereas 100% removal of the thickness was only noted for the damage classification level 4 (failure in Test 8A and 8B). Damage level 1 stands for statically stable scour protections, which were not considered in this dataset. This information is gathered in Table 2.

Test 8A and 8B are identified as failures for a reference sub-area of $4D_{n50}^2$, *i.e.* den Boon *et al.* (2004) criterion is mathematically verified. The maximum S_{3D} obtained was 5.6 in both tests, with overlapping sub-areas as in Figure 1. In this particular case, as the geotextile filter was used the S_{3D} development stops once the filter is achieved. In case of a granular sand filter, the S_{3Dsub} may increase until the scour hole reaches its equilibrium. It is interesting to note that the number of sub-areas with total removal of the scour protection increased from 48 to 73 occurrences, corresponding to exposed areas of sand-bed of 0.35% and 0.45% of the total area of the protection ($A_{protection}$=1.70 m^2). Inspection of the damage locations in the right hand panels of Figure 2 and 3 show material has moved from one test to the next due to waves and currents An important aspect is that, for the analysed tests, the den Boon *et al.* (2004) visual criteria finds a good agreement with the bathymetric analysis hereby presented and that identifies Test 8 as a failure. The same can be said to the association of the visual damage levels from De Vos *et al.* (2012) and the thickness reductions given in Table 1.

Table 1. Number of $A_{sub}=4D_{n50}^2$ vs. % of thickness reduction, n=number of equivalent layers of rock material with size D_{n50} and visual damage level as defined in De Vos *et al.* (2012).

Test	n	N	D_{n50}	Number of sub-areas	Visual damage level	Nº of sub-areas with % of thickness reduction			
	[D_{n50}]	[waves]	[mm]	[-]	[-]	25%	50%	75%	100%
Test04A	2.8	1000	12.5	65164	3	2349	372	60	0
Test04B		3000	12.5	65164	3	4789	823	75	0
Test08A	5.6	1000	6.75	66432	4	2926	1985	674	48
Test08B		3000	6.75	66432	4	5195	2669	960	73
Test10A	9	1000	6.75	66432	2	83	0	0	0
Test10B		3000	6.75	66432	2	278	0	0	0
Test12A	8.1	1000	13.5	265716	3	8045	24	0	0
Test12B		3000	13.5	265716	3	13560	1901	48	0
Test13A	8.2	1000	13.5	265716	2	1695	0	0	0
Test13B		3000	13.5	265716	3	3719	355	0	0

Table 2. Visual damage number vs. % of thickness reduction.

Visual Damage Level (interpreted stability)		% of thickness reduction
1	no movement of the stones (static stability)	0%
2	very limited movement of stones (dynamic stability)	$0 < x \leq 25\%$

3	significant movement of the stones, without failure of the protection (dynamic stability)	$25 < x \leq 75\%$
4	failure	$75 < x \leq 100$ %

As explained in Fazeres-Ferradosa *et al.* (2019), the range of values obtained with $A_{sub}=4D_{n50}^2$ has no direct relationship with the range obtained in De Vos *et al.* (2012) since, the considered area largely affects the range of S_{3D}. However, its physical interpretation is the same. Test 8 was performed with an equivalent number of 5.6 layers of stones with a D_{n50}=6.75 mm, *i.e.* thickness of the protection is equal to $n \times D_{50}=5.6D_{n50}$. If the S_{3Dsub} reaches the reference value 5.6 for a certain sub-area, then the scour protection over an area of $4D_{n50}^2$ was completely removed and the geotextile is exposed. Figures 2 and 3 provide the digital terrain models for the scour protection derived from the bathymetry for Test 8 and the sub-areas associated with the 100% removal of the scour protection, *i.e.* failure occurrence generally defined as the $S_{3Dsub} \geq 5.6$, which in this case, with the existence of geotextile, becomes $S_{3Dsub}=5.6$.

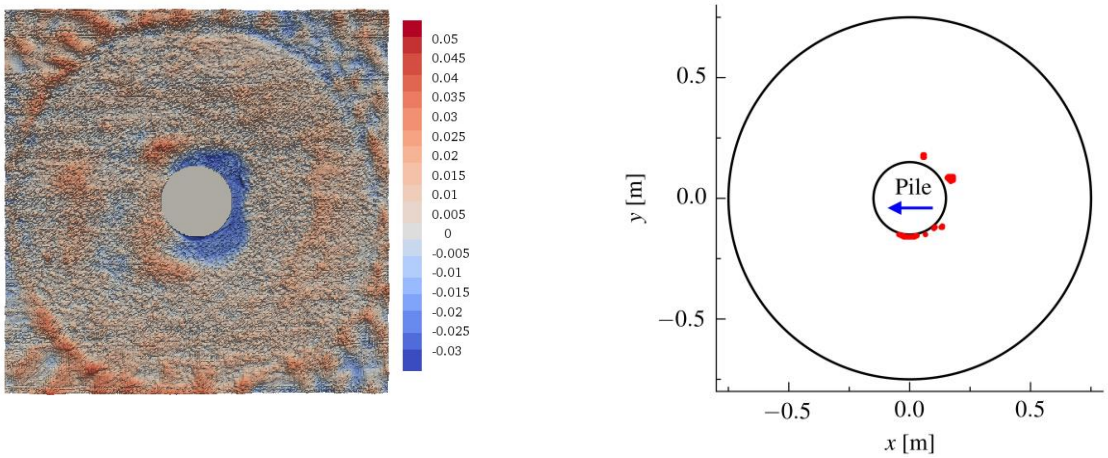

Figure 2. Left: digital terrain model for Test 8A with differences Δ in bed elevation (m). Right: Sub-areas with size $4D_{n50}^2$ that registered the exposure of the geotextile. Current from right to left and waves opposing current.

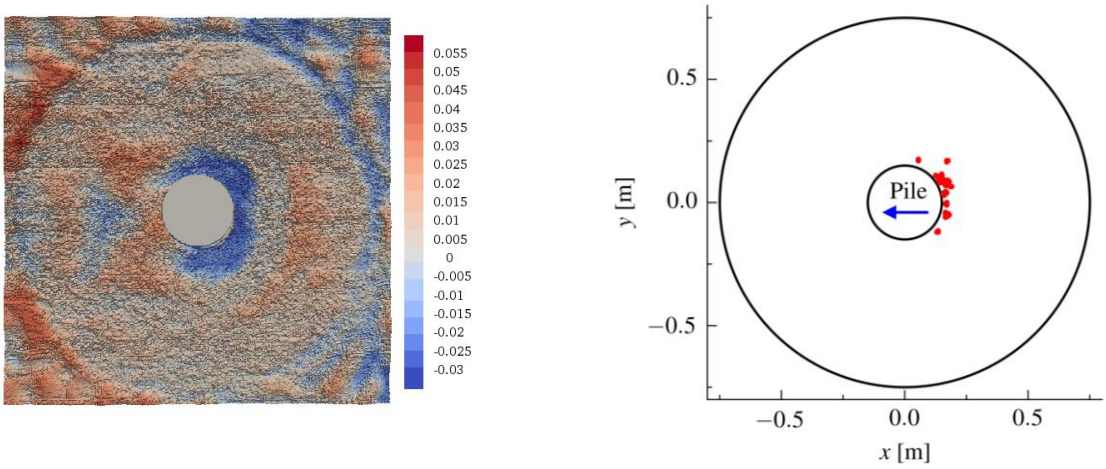

Figure 3. Left: digital terrain model for Test 8B with differences Δ in bed elevation (m). Right: Sub-areas with size $4D_{n50}^2$ that registered the exposure of the geotextile. Current from right to left and waves opposing current.

The set of tests introduced by De Vos *et al.* (2012) only includes protections with thicknesses of $2.5D_{n50}$ and $3D_{n50}$. For that set, analysed with A_{sub} equal to the monopile cross-section, tests with a value of S_{3D} above 1.0 but still smaller than 2.5 and 3.0 were identified as failures (see for example Tests nº 3, 4, 38, 51 and 52 from De Vos *et al.*, 2012). This does not occur in the present data set. Test 8 was the only one registering S_{3Dsub} equal to its equivalent number of layers, *i.e.* above 5.6.

Although the analysis of a larger data set is required for a proper generalization of the conclusions here presented, the use of areas with size of $4D_{n50}^2$ seems suitable to analyse failure according to the S_{3D} interpretation proposed in the previous section.

The use of smaller areas allows for a larger sample of overlapping values of S_{3Dsub} which in turn allow for a perception on the relevance of a particular value of S_{3Dsub} in the overall damage occurring at the protection. Figure 4 provides the empirical cumulative distribution function of damage, hereby called the damage distribution, occurring for Test 8A and 8B. In this case, only cases with $S_{3Dsub}>0$ are plotted, for a better perception of damage differences between 1000 and 3000 waves.

It is possible to see that, as the waves and currents progress from the end of one test to the next, the curve gets slightly flattened. Hence meaning that the same quantile of damage corresponds to a larger damage number. In other words, larger damage numbers have a higher probability of exceedance.

In addition, the vertical line corresponding to the failure domain is plotted, i.e. the vertical line at $S_{3Dsub}=5.6$. Results also show that the use of smaller sub-areas enables a complementary analysis to the maximum S_{3D} value. Hence it becomes possible to understand if a particular maximum S_{3D}, formerly used in the literature to identify the failure, is isolated or if it corresponds to a lower quantile in the distribution, thus meaning that it is more likely to be exceeded.

On the other hand, if small sub-areas are used, it is important to relate them with sizes that may allow for a physical interpretation of the results, such as the $4D_{n50}^2$ criterion given in den Boon *et*

al. (2004). Although not allowing for such a large sample of damage numbers on the scour protection area, it is noted that the sub-areas used in De Vos *et al.* (2012) find a meaningful interpretation in the fact that the cross-section of the pile is easily related with the Keulegan Carpenter and the pile Reynolds numbers (Whitehouse, 1998), which are governing parameters of scour phenomena at marine foundations.

If Tests 8A and 8B are analysed with non-overlapped sub-areas equal to the cross-section of the monopile, the maximum damage numbers are 2.01 and 2.47, respectively. If these are interpreted as the number of stone layers that were removed over the area of $A_{sub}=\pi\times(D_p)^2/4$, then the scour protection would be regarded as a non-failure case. This highlights the need for further research regarding the association of the failure interpretation for sub-areas of different sizes. For scour protections with thicknesses outside the range tested in De Vos *et al.* (2012), the use of the sub-areas equal to $4D_{n50}^2$ might be helpful as they allow for the identification of specific regions for which the sand bottom or the filter layer were exposed.

This representation might be used in future definitions of a possible failure criteria based on the statistical distribution of damage. Nevertheless, such a step still requires the analysis of a larger data set.

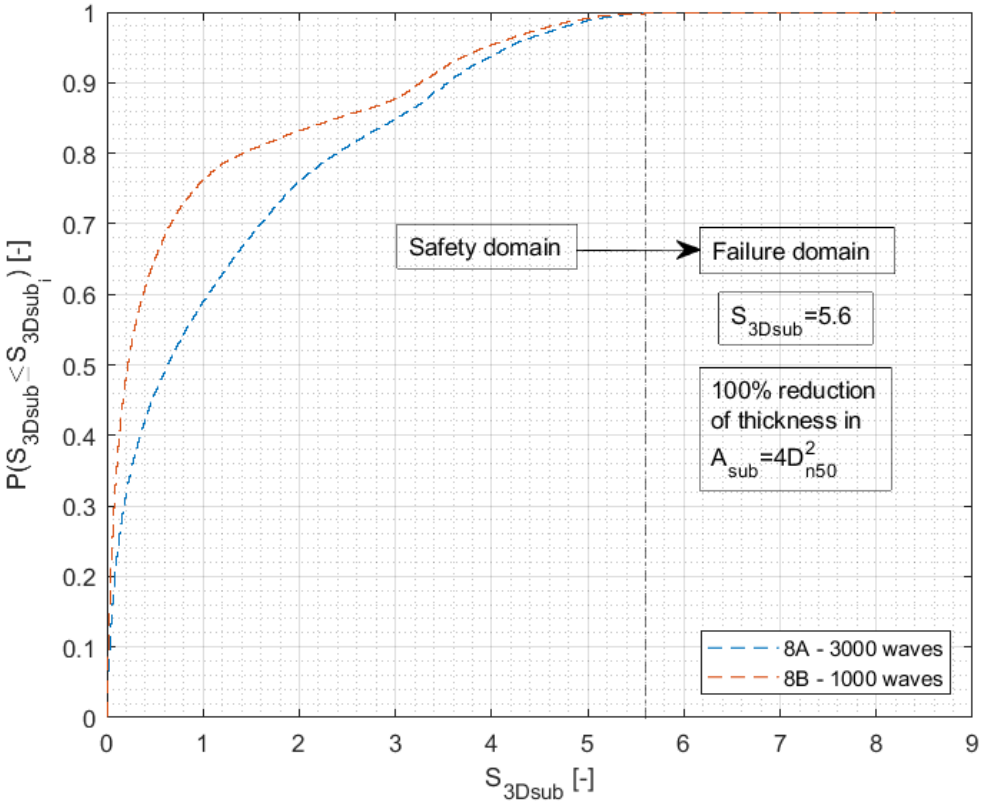

Figure 4. Damage distribution of S_{3Dsub} registered in Test 8A and 8B, with the threshold for failure definition and $A_{sub}=4D_{n50}^2$.

CONCLUSION

A set of scour protection tests from the PROTEUS project were analysed, with a focus on the discussion of failure for tests with different thicknesses of placed rock material (with nominal

diameter D_{n50}). A methodology based on overlapping sub-areas with a size of $4D_{n50}^2$ was used to assess the thickness reduction at the protection and to compare it with the damage number interpreted as the number of layers of stones, with size D_{n50}, that were removed over the sub-area. Under this interpretation only Tests 8A and 8B were identified as failures. The following conclusions were derived from the present research:

- Analysis of Tests 8A and 8B allowed for the exact identification of the den Boon *et al.* (2004) criterion based on bed elevation differences, confirming the presence of sub-areas of $4D_{n50}^2$ with total removal of the protection.
- A good agreement was found between the percentage of thickness reduction and the visual damage levels defined by De Vos *et al.* (2012) – Table 2.
- Damage distributions of S_{3Dsub} can be compared with the number of equivalent layers of stones, with size D_{n50}, in order to analyse the quantile for which failure occurred. This allows for a complementary analysis of damage behaviour rather than just looking at the maximum S_{3D}.
- As damage increases the damage distribution tends to flatten, *i.e.* larger values of S_{3D} appear for lower quantiles of the distribution, thus being more likely to be exceeded.
- The range of damage numbers increases when using the den Boon *et al.* (2004) reference area when compared to the one used in De Vos *et al.* (2012).
- Damage calculation with $A_{sub}=4D_{n50}^2$ is recommended for the analysis of filter/sand exposure at marine scour protections.

Future work should extend this data set to include more cases identified as failure. This would allow for a better testing of the present method's accuracy. Further research is required for a better understanding of the relationship between the damage numbers based on overlapping sub-areas and the ones formerly introduced in De Vos *et al.* (2012). The main goal of future developments should be focused on the definition of failure criteria that accounts for the damage distribution and that couples such distribution with the filter/sand exposure.

ACKNOWLEDGEMENTS

The work described in this publication was supported by the European Community's Horizon 2020 Research and Innovation Program through the grant to HYDRALAB-PLUS, Contract no. 654110. Fazeres-Ferradosa was supported by the project POCI-01-0145-FEDER-032170 (ORACLE project), funded by the European Fund for Regional Development (FEDER), through the COMPETE2020, the Programa Operacional Competitividade e Internacionalização (POCI) and FCT/MCTES through national funds (PIDDAC).

REFERENCES

Chavez, C.E.A., Stratigaki, V., Wu, M., Troch, P., Schendel, A., Welzel, M., Villanueva, R., Schlurmann, T., De Vos, L., Kisacik, D., Pinto, F.T., Fazeres-Ferradosa, T., Santos, P.R., Baelus, L., Szengel, V., Bolle, A., Whitehouse, R., and Todd, D. (2019). "Large-Scale

Experiments to Improve Monopile Scour Protection Design Adapted to Climate Change—The PROTEUS Project." *Energies,* 12(9), 1709. doi:10.3390/en12091709

De Vos, L., De Rouck, J., Troch, P., and Frigaard, P. (2012). "Empirical design of scour protections around monopile foundations - Part 2 - Dynamic approach." *Coastal Engineering,* 60, 286-298. doi:10.1016/j.coastaleng.2011.11.001

den Boon, J. H., Sutherland, J., Whitehouse, R., Soulsby, R., Stam, C. J., Verhoeven, K., and Hald, T. (2004). "Scour behaviour and scour protection for offshore monopile foundations of offshore wind turbines." *(EWEC) European Wind Energy Conference & Exhibition. London: EWEA.*

Fazeres-Ferradosa, T., Taveira-Pinto, F., Romão, X., Vanem, E., Reis, M.T., and das Neves, L. (2018a). "Probabilistic design and reliability analysis of scour protections for offshore windfarms." *Engineering Failure Analysis*, 91, 291-305, doi:10.1016/j.engfailanal.2018.04.035.

Fazeres-Ferradosa, T., Taveira-Pinto, F., Reis, M. T., and das Neves, L. (2018b). "Physical modelling of dynamic scour protections: Analysis of the Damage Number. " *Proceeding of the Institution of Civil Engineers - Maritime Engineering,* 171(1), 11-24. doi:https://doi.org/10.1680/jmaen.2017.26

Fazeres-Ferradosa, T., Taveira-Pinto, F., Rosa-Santos, P., and Chambel, J. (2019). "Reliability Analysis of Offshore Scour Protections – Review of scientific and technical challenges. " *Proceedings of the Institution of Civil Engineers - Maritime Engineering*, 172(3), 104-117. doi:10.1680/jmaen.2019.11

Mayall, R.O., Byrne, B.W., Burd, H.J., McAdam, R.A., Cassie, P. and Whitehouse, R.J.S. (2019). "Modelling of foundation response to scour and scour protection for offshore wind turbine structures." *Scour and Erosion IX : Proceedings of the 9th International Conference on Scour and Erosion (ICSE 2018), November 5-8, 2018, Taipei, Taiwan* (Ed. Keh-Chia, Y).

Schendel. A., Goseberg, N., Schlurmann, T. (2018). "Influence of reversing currents on the erosion stability and bed degradation of widely graded grain material". *International Journal of Sediment Research*, Vol. 33, pp. 68-83

Whitehouse, R. (1998). "*Scour at Marine Structures: A Manual for Practical Applications*." Thomas Telford. London.